Journal of Experimental Marine Biology and Ecology 486 (2017) 188–194

Contents lists available at ScienceDirect

Journal of Experimental Marine Biology and Ecology

journal homepage: www.elsevier.com/locate/jembe

Branches and plates of the morphologically plastic coral *Porites rus* are insensitive to ocean acidification and warming

Elizabeth A. Lenz [a,b,*], Peter J. Edmunds [b]

[a] Hawaii Institute of Marine Biology, University of Hawaii, PO Box 1346, Kāneohe, HI 96744, USA
[b] Department of Biology, California State University, Northridge, 18111 Nordhoff Street, Northridge, CA 91330-8303, USA

ARTICLE INFO

Article history:
Received 3 April 2016
Received in revised form 3 October 2016
Accepted 5 October 2016
Available online 18 October 2016

Keywords:
Scleractinians
Skeletal morphology
Climate change
Mo'orea
French Polynesia

ABSTRACT

This study tested the hypothesis that intraspecific morphological plasticity within a scleractinian coral elicits differential responses to elevated P_{CO2} and temperature. In Mo'orea, French Polynesia, two short-term laboratory experiments (21 and 14 days) were conducted to test the effects of P_{CO2} (400 vs. 700 μatm), and P_{CO2} (400 vs 1000 μatm) combined with temperature (27.0 vs. 29.8 °C), on branches and plates of *Porites rus*. Experiments employed two irradiances (~1000 vs 200 μmol photons m^{-2} s^{-1}), which characterized the microenvironments on the shallow fringing reefs where branching and plating morphologies are common, respectively. Calcification of both morphologies was insensitive to P_{CO2}, as well as the combined effects of elevated P_{CO2} and temperature. Mean calcification rates were faster in high light than in low light for both morphologies, and biomass was greater in plates than branches in all treatments. Together, our results suggest *P. rus* is robust to increased P_{CO2} and high temperature within the constraints of the treatments applied. Morphological plasticity in this species does not mediate physiological resistance to low pH and high temperature.

1. Introduction

Multiple chronic and acute disturbances are threatening tropical scleractinians (De'ath et al., 2012; Jackson et al., 2014), ultimately reducing the ecological resilience (sensu Holling, 1973) of coral reef ecosystems (Bellwood et al., 2004; McClanahan et al., 2002). One of the major chronic disturbances affecting corals is ocean acidification (OA) (Hoegh-Guldberg et al., 2007; Albright et al., 2016), which is the reduction in oceanic pH as a result of atmospheric carbon dioxide (CO_2) dissolving in seawater (Doney et al., 2009). OA changes the concentration of dissolved inorganic carbon (DIC) species in seawater, and reduces the aragonite saturation state, which plays an important role in determining the rate of coral calcification (Cohen and Holcomb, 2009) and reef accretion (Feely et al., 2009; Silbiger et al., 2014). Varied physiological responses to elevated P_{CO2} have been identified both within and among coral taxa (Comeau et al., 2013a, 2014; Kroeker et al., 2010, 2013; Okazaki et al., 2016), which emphasizes the spectrum of sensitivities of corals to reduced pH. Mechanisms supporting higher resistance of individual corals to OA remain largely unknown (Anthony et al., 2008; Cohen and Holcomb, 2009; Comeau et al., 2013a, 2014).

Inter- and intra- specific variation in the sensitivity of scleractinians to OA may be associated with aspects of skeletal phenotype, including skeletal porosity and rate of $CaCO_3$ deposition (Chan and Connolly, 2013; Comeau et al., 2014; Tambutté et al., 2015). Features of the coral holobiont, such as corallum morphology and rates of calcification, have been used in previous studies to distinguish functional groups of corals based on their sensitivity to OA, but the distinction in sensitivity between groups has been equivocal (Comeau et al., 2013a, 2014; Darling et al., 2012; Edmunds, 2011). In natural environments and manipulative studies, mounding corals, such as massive *Porites* spp., are more resistant to elevated P_{CO2} up to 2000 μatm, and temperatures as high as 30 °C, compared to some branching corals, such as *Acropora* spp. and *Pocillopora* spp. (Adjeroud et al., 2009; Comeau et al., 2014; Loya et al., 2001; van Woesik et al., 2011). Organizing corals into functional groups may be helpful in identifying responses to environmental stressors.

Comeau et al. (2014) tested the effects of OA on corals categorized into three functional groups based on: 1) corallum morphology, 2) skeletal porosity, and 3) speed of calcification (e.g., fast vs. slow). After corals were exposed to ~2000 μatm P_{CO2} for 2 weeks, they found that calcification rates of "fast-growing" corals (*Acropora pulchra* and *Psammacora profundacella*) declined, whereas slow-growing corals (*Porites irregularis* and *Pocillopora damicornis*) were unaffected. While Comeau et al. (2014) did not find a strong association between corallum morphology and sensitivity to OA, Anthony et al. (2008) found there

* Corresponding author at: Hawaii Institute of Marine Biology, University of Hawaii, PO Box 1346, Kāneohe, HI 96744, USA.
E-mail address: ealenz@hawaii.edu (E.A. Lenz).

http://dx.doi.org/10.1016/j.jembe.2016.10.002
0022-0981/

was higher sensitivity in branching (*A. intermedia*) versus massive (*P. lobata*) coral. The opposing conclusions by these two studies may reflect the use by Comeau et al. (2014) of an experimental design in which species was used as a random factor nested with a contrast of morphology, and thus intrinsic differences between species may have reduced the statistical power of detecting an effect of morphology. Potentially, the results of a test for morphology might be more effective if it was accomplished using a single species that produced multiple morphologies through phenotypic plasticity (e.g., Todd, 2008). To gain further insight into the responses of corals to OA (Comeau et al., 2014; Darling et al., 2012; Edmunds et al., 2014), it might therefore be valuable to consider coral species that are plastic in select traits (e.g., morphology) to test the role of variation within these traits in determining the extent of intraspecific responses to OA.

For this study, two laboratory experiments were conducted to test the hypothesis that corallum morphology in *Porites rus* mediates the response to elevated P_{CO2} and seawater temperature. *P. rus* was selected because it is morphologically plastic, and produces branches and plates within a single colony (Jaubert, 1977; Padillo-Gamiño et al., 2012). In Mo'orea, French Polynesia, where this study was conducted, *P. rus* is abundant in shallow water (<4-m depth) where coral cover in 2012 (when this study was completed) was as high as 28% on fringing reefs along the north shore (Adjeroud and Salvat, 1996; Jaubert, 1977; Padillo-Gamiño et al., 2012); *P. rus* represented ~27–100% of this coral cover (Edmunds, 2016). Morphological plasticity in *P. rus* is largely driven by light (Jaubert, 1977; Padillo-Gamiño et al., 2012), with branches forming in habitats with high light intensities, and plates forming in habitats with low light intensities (Fig. 1).

Experiment 1 tested the response of branches and plates to P_{CO2} values expected to occur by 2100 under representative concentration pathway (RCP) scenario 6.0 (700 μatm), which posits mitigation of fossil fuel production by 2100 (Moss et al., 2010). Experiment 2 compared the response of both morphologies to elevated P_{CO2} predicted to occur by 2100 under a more stringent scenario defined by RCP scenario 8.5 (1000 μatm), which represents a worst-case scenario for the end of the current century (RCP Scenario 8.5; Moss et al., 2010). Additionally, in the second experiment, P_{CO2} treatments were crossed with a temperature treatment that contrasted ambient (27.2 °C) with a temperature 2 °C above ambient, as predicted to occur by 2100 (29.8 °C) (Hoegh-Guldberg et al., 2007). A light treatment was added to both experiments to test for effects of the physical environment on the reef where the two morphologies are found (e.g., Jaubert, 1977), and to avoid generating a bias in the response of a morphology type to the P_{CO2} and temperature treatments.

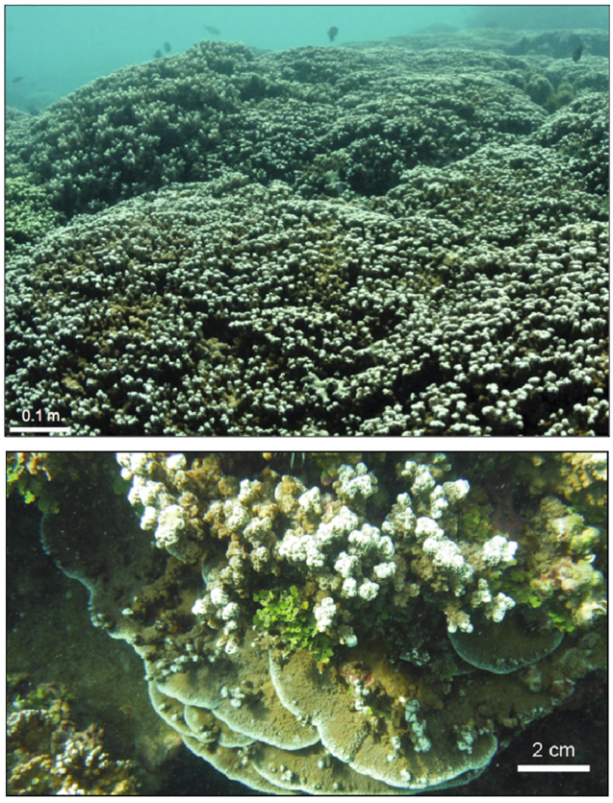

Fig. 1. Branches (top) and plates (bottom) of *Porites rus* in Mo'orea, French Polynesia. Pictures were taken on the fringing reef at 0.5-m depth in 2012.

2. Materials and methods

2.1. Coral collection and acclimation

For each experiment, branches and plates of *Porites rus* were collected haphazardly at 0.5–2.0 m depth along a fringing reef in Cook's Bay, Mo'orea (17°48.96S, 149°81.88 W). Individual branches and plates were placed in plastic bags and brought to the Richard B. Gump South Pacific Station in a cooler filled with seawater. At the lab, branches were trimmed to 3-cm length, and plates to 3-cm width, and attached to plastic bases with marine epoxy (Z-Spar A-788 Splash Zone Compound Los Angeles, CA, USA) in either an upright or horizontal position, respectively. After allowing the epoxy to cure for 48 h under high flow, corals were transferred to a 1000 L acclimation tank for 1 week, in which they were exposed to similar conditions to those employed in the subsequent mesocosm experiment. The acclimation period was intended to reduce stress induced from collection and handling, and to allow corals to acclimate to the incubation conditions prior to the start of the experiment.

P_{CO2} and temperature in the acclimation tank were maintained at ambient conditions in Cook's Bay when the experiments were conducted (~400 μatm P_{CO2} for both experiments, 27 °C for Experiment 1 in April–May 2012, and 28 °C for Experiment 2 in January–February 2013). Branches and plates were evenly distributed throughout the circular acclimation tank, either in the center or the perimeter of a circular table that rotated at two revolutions d^{-1} beneath four 75-W Light-Emitting Diode lamps (Aquallumination® LED System Model: Sol Blue, Ames, IA). The LED lamps operated on a 12:12 h light:dark photoperiod with irradiance gradually increasing from 0 to 100% of maximum irradiance, remaining at 100% for 4 h, and reducing in intensity over the final 4 h of the day to simulate field conditions. Maximum light intensities were ~300 μmol photons m^{-2} s^{-1} and ~700 μmol photons m^{-2} s^{-1} (measured with 4π quantum sensor [LI-193] and a LiCor LI-1400 m) at the perimeter and center of the tank, respectively. These positions were used to mimic high and low light intensity habitats on the fringing reefs of Mo'orea where branches and plates of *P. rus* are most common, respectively. Mean maximum light intensities in the habitats from which the corals were collected were measured close to noon on sunny days in April. Light intensities were measured using two MkV-L logging light sensors (JFE Advantech Co., Kobe, Japan) each equipped with a 4π spherical quantum PAR sensor, and placed at 0.5 m and 2.0 m depth in high and low light environments where branches and plates were collected. The sensors recorded light in 10 min intervals over 2 d (27–28 April 2012). Mean values of light intensities between 11:00–13:30 h were 1472 ± 92 μmol photons m^{-2} s^{-1} where branches were collected, and 226 ± 7 μmol photons m^{-2} s^{-1} where plates were collected (±SE, $n = 64$; Fig. 2).

2.2. Seawater carbonate chemistry and tanks

Tanks used for both experiments contained 150 L of filtered seawater (passed through a sand filter) that was supplied continuously (200

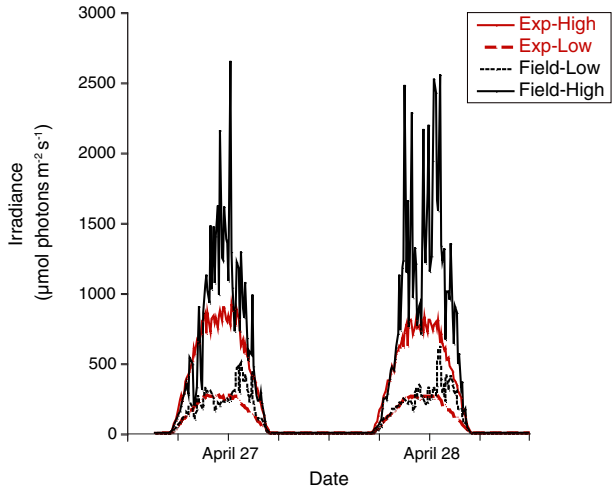

Fig. 2. Light (μmol photons m^{-2} s^{-1}) measured over 2 d in 2012 in tanks (high light intensities during the experiment [Exp-High] and low light intensities during the experiment [Exp-Low]) and in the natural environment where branches and plates of *P. rus* were collected at 0.5 and 2.0 m depth, respectively (high light [Field-High] and low light [Field-Low] in the field).

mL min^{-1}). Each tank was equipped with a temperature controller and LED lamp, identical to the ones used in the acclimation tank, which were used to create high and low light conditions (described below). Ambient P_{CO2} (400 μatm) was maintained through direct bubbling of ambient air into the tanks, and elevated P_{CO2} (Experiment 1: 700 μatm and Experiment 2: 1000 μatm) was generated by mixing enriched CO_2 and ambient air with a solenoid-controlled gas regulation system (Model A352, Qubit, Ontario, Canada).

Temperature, pH, total alkalinity (A_T), and salinity were monitored throughout the experiment to characterize seawater carbonate chemistry (Table 1). Temperature and pH were measured twice daily (08:00 h and 18:00 h), A_T was assessed every other day by sampling 250 mL of seawater from each tank, temperature was measured daily with a digital thermometer (Fisher Scientific model 15-077-9; accuracy ±0.01 °C), and salinity was measured daily with a YSI 3100 Conductivity Meter (YSI Inc., Yellow Springs, OH, USA). Seawater pH_T and total alkalinity (A_T) were calculated from titrations using the gran function in an open-cell potentiometric automatic titrator (T50, Mettler-Toledo International Inc., Columbus, OH, USA) fitted with a DG115-SC pH probe that was calibrated with TRIS buffer (A. Dickson, Scripps Institution of Oceanography). Standard operating procedures 3b (Dickson et al., 2007) were followed and A_T of certified reference materials (Dickson Laboratory, Scripps Institution of Oceanography) was determined prior to seawater titrations, which provided values ±3.0 μmol kg^{-1} (Batch 108, $n = 10$) of certified values. Carbonate seawater chemistry (P_{CO2}, HCO_3^-, CO_3^{-2}, aragonite saturation state [Ω_{Arag}], and DIC) was calculated using A_T (μmol kg^{-1}), pH, salinity, and temperature with the R software package "seacarb" (Lavigne and Gattuso, 2012).

2.3. Experiment 1

Experiment 1 tested the effects of high P_{CO2} on branches and plates of *Porites rus* over 21 d in April–May 2012, with the P_{CO2} treatment selected to represent conservative predictions for atmospheric levels of CO_2 by the end of the current century (700 μatm; RCP Scenario 6). There were four replicate tanks for each P_{CO2}, and seawater temperature was maintained at 28.0 °C, which was the ambient seawater temperature when the experiment was conducted. Sets of three branches and three plates were placed in the center and along the margin of the 8 tanks, where they received light from LED lamps at mean intensities of 1017 ± 20 μmol photons m^{-2} s^{-1} and 251 ± 7 μmol photons m^{-2} s^{-1}, respectively (±SE; $n = 24$). Light intensities in all tanks were measured weekly with the 4π Li-Cor sensor when the LED lamps reached 100% power (between 10:00 and 14:00 h). Additionally, an MkV-L logging light sensor was placed in the center, with another along the edge, of one representative tank to compare light intensities in the tanks with those recorded in the field using the same sensor (Fig. 2).

2.4. Experiment 2

Experiment 2 was conducted for 14 d from January–February 2013, and tested the effects of elevated P_{CO2} and temperature at different light intensities on branches and plates of *P. rus*. The high P_{CO2} treatment was targeted at 1000 μatm, as it is a more stringent treatment than applied in Experiment 1. P_{CO2} treatments were crossed with two temperatures (27.2 °C and 29.8 °C) that provided exposure to the ambient seawater temperature when the experiment was conducted, and +3 °C above ambient seawater temperature when the experiment was conducted, respectively. Two tanks were assigned to each of four treatments: ambient temperature-ambient P_{CO2} (AT-ACO_2), ambient temperature-high P_{CO2} (AT-HCO_2), high temperature-ambient P_{CO2} (HT-ACO_2), high temperature-high P_{CO2} (HT-HCO_2). Mean light intensities in the tanks were reduced to 728 ± 30 μmol m^{-2} s^{-1} and 154 ± 4 μmol m^{-2} s^{-1} (±SE, $n = 8$) to prevent paling of the corals, which was observed in plates under high light during the first experiment. Light intensities were reduced by placing neutral density mesh over half of each tanks. Three branches and three plates of *P. rus* were placed in both the high and low light treatments within each tank, and were repositioned every other day within each treatment to avoid position effects.

2.5. Calcification rates and biomass

In both experiments, calcification and tissue biomass were used to determine the effect of treatments on the branches and plates of *P. rus*. Calcification was measured by buoyant weighing (Davies, 1989) corals at the beginning and end of each experiment, with the difference between the two used to calculate the change in dry weight using the density of aragonite (2.93 g cm^{-3}). The dry weight increment was normalized to time and the tissue area of the coral, as estimated using aluminum foil (Marsh, 1970) (units of mg cm^{-2} d^{-1}).

Tissue biomass was also measured as an indicator of coral health in the two morphologies. Biomass was measured by fixing corals in 10%

Table 1
Summary of seawater carbonate chemistry in Experiment 1 in which 8 tanks were assigned randomly to four treatments of ACO_2 = ambient P_{CO2} and HCO_2 = high P_{CO2} for 21 d ($n = 74$) and Experiment 2 in which 8 tanks were assigned randomly to four treatments designated as AT-CO_2 = ambient temperature ambient P_{CO2}, HT-ACO_2 = high temperature ambient P_{CO2}, AT-HCO_2 = ambient temperature high P_{CO2}, HT-HCO_2 = high temperature high P_{CO2} for 21d ($n = 36$). Mean ± SE (SE not shown when <0.01).

	Treatment	Temperature (°C)	Salinity	pH	A_T (μmol kg^{-1})	P_{CO2} (μatm)	$\Omega_{Aragonite}$
Experiment 1	ACO_2	27.99 ± 0.02	36.1	8.07	2335 ± 1	374 ± 3	3.97 ± 0.02
	HCO_2	28.01 ± 0.02	36.1	7.84	2332 ± 1	712 ± 8	2.64 ± 0.02
Experiment 2	AT-ACO_2	27.32 ± 0.04	35.3	8.06	2313 ± 2	379 ± 3	3.78 ± 0.02
	HT-ACO_2	29.82 ± 0.05	35.3	8.03	2317 ± 2	406 ± 2	3.92 ± 0.02
	AT-HCO_2	27.05 ± 0.05	35.3	7.67	2316 ± 1	1108 ± 15	1.79 ± 0.02
	HT-HCO_2	29.80 ± 0.04	35.3	7.67	2318 ± 2	1107 ± 16	1.99 ± 0.02

formalin, decalcifying in 5% HCl, removing endolithic algae and sponges with forceps, and determining the dry weight of the tissue as described below. In Experiment 1, decalcified tissue was homogenized by sonication in freshwater to produce a slurry (which was necessary for analyses in a separate study), and duplicate aliquots were dried to a constant weight for 48 h at 60 °C. In Experiment 2, the entire decalcified tissue was rinsed in freshwater and dried to a constant weight at 60 °C for 72 h. Tissue biomass was normalized to surface area (mg cm^{-2}) to evaluate treatment effects on this variable.

2.6. Statistical analysis

In Experiment 1, calcification and biomass were initially analyzed using a 4-way partly nested split-plot ANOVA, in which P_{CO2} was the fixed between plot-effect, morphology, and light intensity were fixed split-plot effects, and tank was treated as the plot (a random effect nested within treatments) (Table 2A). In Experiment 2, calcification and biomass were analyzed using a 5-way partly nested split-plot ANOVA, with P_{CO2} and temperature as the fixed between plot-effects, morphology and light intensity were split-plot effects, and tank was treated as plot (a random effect nested within treatments) (Table 2B). In both experiments, tank (as a nested effect), and all other main effects and their interactions were removed sequentially from the statistical model when not significant at $P \geq 0.25$ (Quinn and Keough, 2002), which allowed for the utilization of reduced models in the final analyses. Statistical analyses were performed using Systat 13 running in a Windows environment. Assumptions of normality and homoscedasticity were tested by graphical inspection of residuals.

3. Results

3.1. Experiment 1

3.1.1. Seawater carbonate chemistry

Mean P_{CO2} values across the four ambient P_{CO2} tanks (ACO_2) were maintained at 374 ± 3 μatm, and at 712 ± 8 μatm across the four elevated P_{CO2} tanks (HCO_2) (±SE, $n = 160$; Table 1). Mean temperature pooled among tanks was 28.00 ± 0.03 °C (mean ± SE, $n = 320$). Mean light intensity for the high light treatment was 1017 ± 20 μmol photons m^{-2} s^{-1} and for low light treatment it was 251 ± 7 μmol photons m^{-2} s^{-1} (±SE, $n = 24$; Fig. 2). Neither temperature nor P_{CO2} differed between tanks within each treatment ($P \geq 0.165$), and mean light intensities were similar among all tanks ($P = 0.237$).

3.1.2. Response of corals

A majority of the coral fragments appeared healthy during the experiment except for four plates incubated at high light intensity, which turned pale regardless of P_{CO2} treatment and were removed from the analysis. After 21 d, mean area-normalized calcification for plates ranged from 0.45 ± 0.08 mg d^{-1} cm^{-2} (high light, HCO_2) to 0.62 ± 0.05 mg d^{-1} cm^{-2} (low light, HCO_2), and for branches from 0.38 ± 0.03 mg d^{-1} cm^{-2} (low light, ACO_2) to 0.67 ± 0.05 mg d^{-1} cm^{-2} (high light, ACO_2) (±SE, $n = 8$–12). Tank as a nested effect, the two-way interaction of morphology and P_{CO2}, and the three-way interaction were not significant ($P \geq 0.313$), which resulted in the removal of these effects from the model (Table 2A). Mean area-normalized calcification of plates and branches were unaffected by P_{CO2} ($F_{1,86} = 0.579$, $P = 0.446$). There was an effect of light ($F_{1,86} = 6.070$, $P = 0.015$),

Table 2
Results from the reduced model of the 3-way and 4-way partly nested split plot ANOVA for calcification and biomass under experimental conditions for Experiment 1 (A) and Experiment 2 (B), respectively. Interactions were removed from the model when $P \geq 0.250$ (Quinn and Keough, 2002). * Indicates significant effect.

	Effect	SS	df	MS	F-ratio	P
A Experiment 1						
Calcification source						
Among plots	P_{CO2}	0.033	1	0.033	0.579	0.446
Within plots	Light*	0.346	1	0.346	6.070	0.015
	Morphology	0.071	1	0.071	1.246	0.271
	Morphology × Light	0.184	1	0.184	3.228	0.074
	P_{CO2} × Light	0.097	1	0.091	1.726	0.192
	Error	4.853	86	0.057		
Biomass source						
Among plots	P_{CO2}	0.029	1	0.029	0.007	0.990
Within plots	Light	1.001	1	1.001	0.252	0.617
	Morphology*	32.124	1	32.124	8.102	0.006
	Error	348.928	88	3.965		
B Experiment 2						
Calcification source						
Among plots	P_{CO2}	0.065	1	0.065	0.493	0.484
	Temperature	0.391	1	0.391	2.950	0.089
	P_{CO2} × Temperature	0.064	1	0.064	0.482	0.489
Within plots	Light*	1.318	1	1.318	9.952	0.002
	Morphology*	5.139	1	5.139	38.932	<0.001
	Error	11.653	88	0.132		
Biomass source						
Among plots	P_{CO2}	1.516	1	1.515	0.227	0.635
	Temperature	3.827	1	3.824	0.574	0.451
	P_{CO2} × Temperature	25.364	1	25.364	3.805	0.055
Within plots	Light	<0.001	1	<0.001	<0.001	0.994
	Morphology*	383.588	1	383.588	57.527	<0.001
	Morphology × Light	0.003	1	0.003	<0.001	0.983
	P_{CO2} × Morphology	2.735	1	2.735	0.410	0.524
	P_{CO2} × Light	2.235	1	2.235	0.335	0.564
	Light × Temperature	4.495	1	4.495	0.674	0.414
	Morphology × Temperature	0.187	1	0.187	0.028	0.868
	Light × Morphology × P_{CO2}	0.068	1	0.068	0.010	0.920
	Light × Morphology × Temperature	9.602	1	9.602	1.440	0.234
	Light × Temperature × P_{CO2}	0.68	1	0.680	0.102	0.750
	Morphology × Temperature × P_{CO2}	8.176	1	8.176	1.226	0.272
	Light × Morphology × Temperature × P_{CO2}	12.388	1	12.388	1.858	0.177
	Error	526.767	79	6.668		

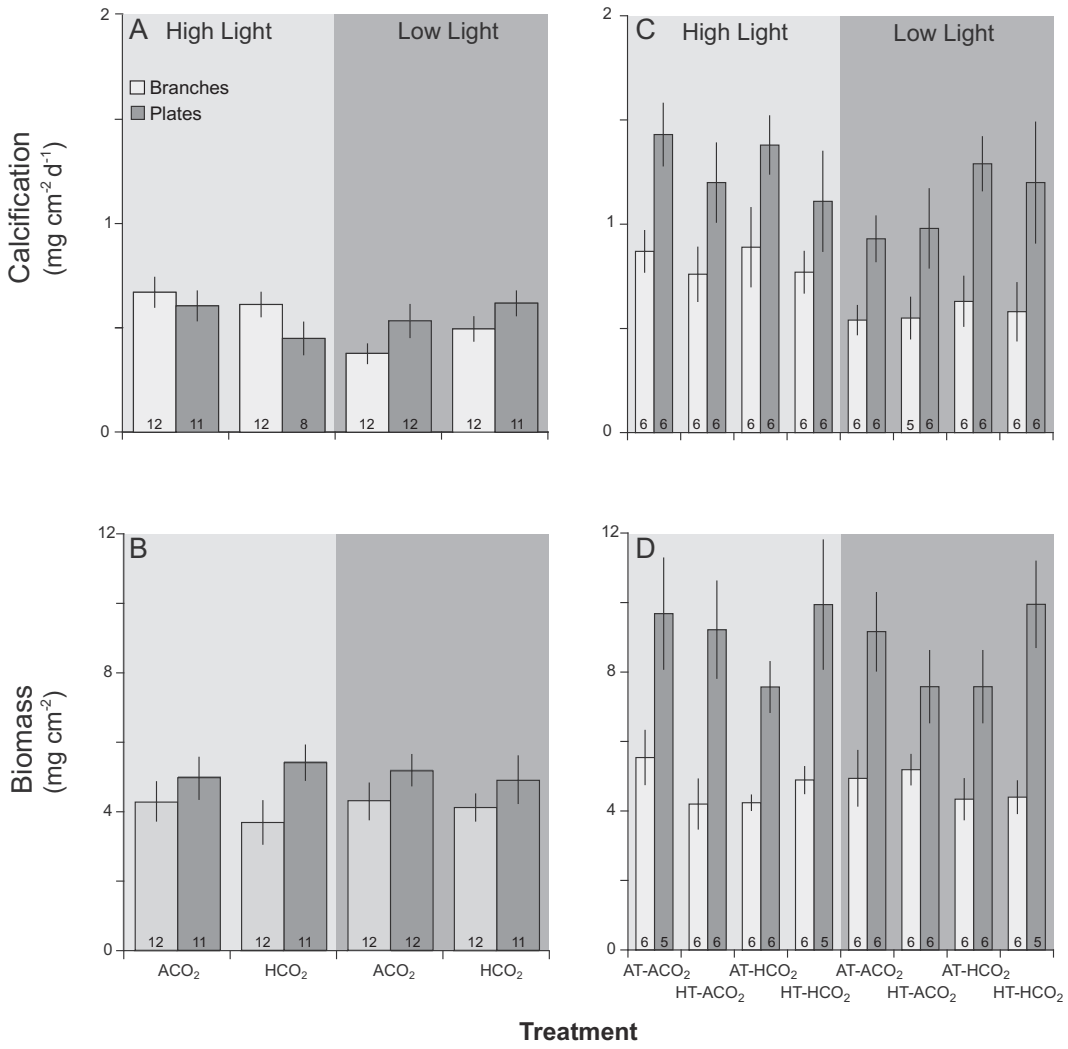

Fig. 3. Mean (±SE) area-normalized calcification (mg cm^{-2} d^{-1}) and tissue biomass (mg cm^{-2}) of branches (light grey) and plates (dark grey) of *Porites rus* from Experiment 1 (A and B) and Experiment 2 (C and D). Branches and plates were incubated under high and low irradiance in ambient (400 μatm, ACO_2) and elevated (700 μatm, HCO_2) P_{CO2} for Experiment 1. In Experiment 2, corals were incubated under ambient temperature-ambient P_{CO2} (AT-ACO_2), high temperature-ambient P_{CO2} (HT-ACO_2), ambient temperature-high P_{CO2} (AT-HCO_2), and high temperature-high P_{CO2} (HT-HCO_2). The number of replicates is shown within each bar (n = 8–12 for Experiment 1 and n = 5–6 for Experiment 2).

with *P. rus* calcifying 26% faster under high light (0.63 ± 0.04 mg day^{-1} cm^{-2}) than low light (0.50 ± 0.03 mg day^{-1} cm^{-2}) (Fig. 3A).

Mean biomass of plates was 5.13 ± 0.28 mg cm^{-2} (±SE, $n = 47$), and for branches was 4.12 ± 0.28 mg cm^{-2} (Fig. 3B; ±SE, $n = 44$). There were no three-way interactive effects of P_{CO2}, light, and morphology ($F_{1,84} = 0.074$, $P = 0.786$) and no two-way interactions ($F_{1,84} \leq 0.912$, $P \geq 0.342$), and therefore, these effects were dropped from the statistical model. Biomass differed between morphologies, with mean biomass 19.4% higher in plates than branches (Fig. 3B; $F_{1,88} = 8.102$, $P = 0.006$). Area-normalized biomass of *P. rus* was not affected by P_{CO2} (Fig. 3B, $F_{1,88} = 0.007$, $P = 0.990$) or light ($F_{1,88} = 0.252$ $P = 0.617$).

3.2. Experiment 2

3.2.1. Seawater carbonate chemistry

Ambient P_{CO2} for the two temperature treatments was 379 ± 3 μatm and 406 ± 2 μatm, while high P_{CO2} was 1108 ± 15 μatm and 1107 ± 16 μatm (all mean ± SE; Table 1). Mean light intensities were 728 ± 24 μmol photons m^{-2} s^{-1} (±SE, n = 8) in the high light treatment, and 154 ± 4 μmol photons m^{-2} s^{-1} (±SE, n = 8) in the low light treatment. Mean ambient temperatures were 27.32 ± 0.04 °C and 27.05 ± 0.05 °C, while mean elevated temperatures were 29.82 ± 0.05 °C and 29.80 ± 0.04 °C (all ±SE; $n = 140$).

3.2.2. Response of corals

The fragments of *Porites rus* appeared healthy and retained dark brown tissue throughout the experiment. After 14 d, mean calcification rates for plates ranged from 0.84 ± 0.25 mg d^{-1} cm^{-2} (high light, HT-HCO_2) to 1.45 ± 0.15 mg d^{-1} cm^{-2} (high light, AT-ACO_2) and 0.54 ± 0.07 mg d^{-1} cm^{-2} (high light, HT-ACO_2) to 1.00 ± 0.18 mg d^{-1} cm^{-2} (high light, AT-ACO_2) for branches (Fig. 3C). Mean calcification rates were unaffected by P_{CO2}, temperature, and the interaction between these factors ($F_{1,78} \geq 0.016$, $P \geq 0.306$), but they differed between light regimes and morphologies (Table 2B). Branches of *P. rus* calcified 41% slower than plates ($F_{1,88} = 38.932$, $P < 0.001$), with mean (±SE) rates of 0.70 ± 0.05 mg d^{-1} cm^{-2} for branches and 1.19 ± 0.06 mg d^{-1} cm^{-2} for plates. Mean calcification rates of fragments despite morphology type were 28% higher under high light than compared to low light conditions ($F_{1,88} = 9.952$, $P = 0.002$), with mean (±SE) rates of 1.05 ± 0.07 mg d^{-1} cm^{-2} under high light and 0.82 ± 0.06 mg d^{-1} cm^{-2} under low light.

Biomass of branches was unaffected by treatments, ranging from 4.20 ± 0.72 mg cm^{-2} (high light AT-HCO_2) to 5.54 ± 0.78 mg cm^{-2} (high light, AT-ACO_2) (both mean ± SE). Plates had 46% more biomass than branches across all treatments ($F_{1,79} = 57.527$, $P < 0.001$), with mean (±SE) values ranging from 7.37 ± 1.48 mg cm^{-2} (HT-ACO_2) to 10.81 ± 1.33 mg cm^{-2} (HT-HCO_2), and for branches, ranging from

4.20 ± 0.72 mg cm^{-2} (AT-HCO_2) to 5.54 ± 0.78 mg cm^{-2} (AT-ACO_2) (Fig. 3D). None of the second, third, or fourth order interactions involving light, temperature, P_{CO2}, and morphology were significant (Table 2B; $F \leq 1.858$, $P \geq 0.177$).

4. Discussion

The purpose of this short-term study was to test for an effect of intraspecific morphological variation on the response of a common reef building coral to OA, either individually or in combination with increased temperature. *Porites rus* was used for this study, as it is an abundant in Mo'orea, and exhibits a high degree of morphological plasticity (Jaubert, 1977) to form branches and plates that are representative of the range of morphologies produced among coral species in most reef habitats (Jackson, 1979). Corallum morphology is a key organismic feature defining much of the structure of coral reef ecosystems, and it plays an important role in creating structural complexity that promotes high diversity through habitat provisioning (Alvarez-Filip et al., 2009; Graham et al., 2006). The capacity for phenotypic plasticity in corallum morphology allows some corals to overcome potential constraints encountered within their environment. Examples of these effects are provided by changes in corallite structure, branch size, and spacing of corallites of the Caribbean coral *Madracis mirabilis* as a function of hydrodynamic exposure and sedimentation (Bruno and Edmunds, 1997), and variation in corallum morphology that reduces diffusion boundary layers and prevents mass transfer limitation of aerobic respiration in multiple coral species (Bruno and Edmunds, 1998; Hoogenboom et al., 2008; Lesser et al., 1994; Patterson, 1992). Corals can respond to environmental gradients through phenotypic plasticity (which includes the capacity for acclimatization), however, the role of plasticity in responding to climate change and ocean acidification is unknown (Edmunds and Gates, 2008; Todd, 2008; Vermeij and Bak, 2002). As seawater pH declines and its temperature rises in coming decades (Doney et al., 2009), it is valuable to test for the potential role of phenotypic plasticity in promoting the persistence of corals under future conditions.

The results from the present study show that branches and plates of *P. rus* were unaffected by 2 to 3 weeks exposure to elevated P_{CO2} (700 μatm), or elevated P_{CO2} (1000 μatm) plus temperature (30 °C). Physiological consequences were associated with morphology, however, with branches having higher calcification rates under high light versus low light intensities, and plates exhibiting similar calcification rates regardless of light intensities, but containing more coral biomass than branches. These results are comparable to findings by Padillo-Gamiño et al. (2012), who described physiological differences between morphologies of *P. rus* in Cook's Bay. Padillo-Gamiño et al. (2012) found that plates had higher photosynthetic rates and potentially lower proportional dependence on heterotrophy as a source of carbon than branches. Despite the aforementioned differences in traits associated with physiological performance of plates and branches of *P. rus*, corallum morphology of *P. rus* in the present study did not affect the sensitivity to elevated P_{CO2} or seawater warming, at least at the treatment levels and exposure times employed. Together, these results underscore the potential of *P. rus* to resist the adverse affects of OA and high temperature (Comeau et al., 2013b), and thereby function as a winner (sensu Loya et al., 2001) on future reefs exposed to warmer seawater with lower pH than current conditions.

Previous short-term studies have shown a variety of responses of calcification of *P. rus* branches exposed to elevated P_{CO2} (Comeau et al., 2013a, 2013b; Edmunds et al., 2012). For example, in Mo'orea, Comeau et al. (2013a) demonstrated that the calcification of *P. rus* branches was reduced ~17% by P_{CO2} as high as ~2073 μatm (relative to ambient controls at 385 μatm), while calcification of branches were unaffected at 1036 μatm. In a separate study, Comeau et al. (2013b) used branches of *P. rus* to test the effects of light (~1000 μmol photons m^{-2} s^{-1} and ~215 μmol photons m^{-2} s^{-1}), and feeding under ambient and elevated P_{CO2} (400 and 700 μatm, respectively), and found no differences in calcification across all treatments. The present study suggests that both morphologies of *P. rus* can resist the increases in P_{CO2} that are expected to occur by the end of the current century, at least in short laboratory experiments. This conclusion, however, should be interpreted with caution as the statistical power for detecting the effects of P_{CO2} and the interaction of P_{CO2} with temperature may have been relatively low. Testing for post hoc statistical power in complex ANOVAs is problematic (Hoenig and Heisey, 2001), but insights into the likely power can be gained from consideration of simpler contrasts. For example, in a test of P_{CO2} (400 μatm versus 700 μatm) on calcification of *P. rus*, the power for detecting a treatment effect of 30% of the mean calcification rate of controls (i.e., at 400 μatm P_{CO2}) with a sample size of 43 (the minimum used in Experiment 2) was ~0.65. Such calculations suggest that the sample sizes used herein probably were sufficient to detect strong effects of P_{CO2}. According to Comeau et al. (2013a), *P. rus* has been observed to be sensitive to high P_{CO2} when more stringent conditions are applied. For example, during their short-term experiments, negative effects on calcification in *P. rus* were established between 1000 and 2000 μatm P_{CO2} (Comeau et al., 2013a). Further studies are required to determine the relevance of the present findings to conditions under which branches and plates of *P. rus* will be exposed to increased P_{CO2} and warming for lengthy periods (i.e., as will occur on future reefs). Although varying experimental duration can elicit acclimation or thresholds effects in some taxa upon exposure to intensified P_{CO2} regimes (Form and Riebesell, 2012), evidence to date has not revealed an unequivocal effect of exposure duration on the response of coral calcification to high P_{CO2} (Chan and Connolly, 2013; Kroeker et al., 2013).

It remains unclear how *Porites rus* maintains calcification rates at 1000 μatm P_{CO2} and 29 °C, but leading explanations focus on the microbial consortium (Rosengberg et al., 2007), coral host traits (e.g., the perforate skeleton), environmental history of the holobiont (Padillo-Gamiño et al., 2012; Putnam and Edmunds, 2011), and variation in *Symbiodinium* clades within the host (Berkelmans and Van Oppen, 2006; Putnam et al., 2012). Of these, variation in *Symbiodinium* clades is particularly, pertinent because corals predominantly associated with a single *Symbiodinium* clade (i.e., specifists [Franklin et al., 2011]) are less sensitive to thermal stress than corals containing a mixture of *Symbiodinium* clades (i.e., generalists [Putnam et al., 2012]), and in *P. rus* from back and fringe reef sites in Mo'orea (≤5-m depth), 98% of the *Symbiodinium* were clade C15 in both plates and branches (Padillo-Gamiño et al., 2012), which appears to be the case for most *Porites* spp. in this location (Franklin et al., 2011; Putnam et al., 2012). The detection of only *Symbiodinium* clade C15 in both *P. rus* morphologies implies high host fidelity, and may contribute to the ability of this coral to withstand elevated temperatures (Putnam et al., 2012; van Woesik et al., 2011). Additionally, traits of *P. rus* that include a perforate skeleton (Comeau et al., 2014) and a thick layer of tissue (Padillo-Gamiño et al., 2012) may contribute to its elevated tolerance of high temperature. Together, the results of the present experiments demonstrate that *P. rus* is hardy with respect to the intensity and duration of the treatment conditions tested, and suggest that this species may continue to provide complex reef structure despite seawater warming and acidification expected to occur by the end of the current century.

Acknowledgements

This research was supported by grants from the U.S. National Science Foundation (OCE 04-17412, 10-26851, and 12-36905), CSUN Science and Mathematics Graduate Student Promise Fellowship, and gifts from the Gordon and Betty Moore Foundation. We are grateful to D. Brown, S. Comeau, N. Evensen, V. Moriarty, N. Spindel, and A. Yarid for their assistance in the field. We would also like to thank the anonymous reviewers, S. Shumway, M. Steele, R.C. Carpenter, and E.D. Sanford for their valuable comments on the manuscript. This is contribution number 248 of the California State University, Northridge, Marine Biology Program. **[SS]**

References

Adjeroud, M., Salvat, B., 1996. Spatial patterns in biodiversity of a fringing reef community along Opunohu Bay, Moorea, French Polynesia. Bull. Mar. Sci. 59, 175–187.

Adjeroud, M., Michonneau, F., Edmunds, P.J., Chancerelle, Y., Lison de Loma, T., Penin, L., Thibaut, L., Vidal-Dupiol, J., Salvat, B., Galzin, R., 2009. Recurrent disturbances, recovery trajectories, and resilience of coral assemblages on a south Central Pacific reef. Coral Reefs 28, 775–780.

Albright, R., Caldeira, L., Hosfelt, J., Kwiatkowski, L., Maclaren, J.K., Mason, B.M., Nebuchina, Y., Ninokawak, A., Pongratz, J., Ricke, K.L., Rivlin, T., Schneider, K., Sesboüé, M., Shamberger, K., Silverman, J., Wolfe, K., Zhu, K., Caldeira, K., 2016. Reversal of ocean acidification enhances net coral reef calcification. Nature 531, 362–365.

Alvarez-Filip, L., Dulvy, N.K., Gill, J.A., Côté, I.M., Watkinson, A.R., 2009. Flattening of Caribbean coral reefs: region-wide declines in architectural complexity. Proc. R. Soc. Lond. B 276, 3019–30125.

Anthony, K.R.N., Kline, D., Diaz-Pulido, G., Dove, S., Hoegh-Gulberg, O., 2008. Ocean acidification cause bleaching and productivity loss in coral reef builders. Proc. Natl. Acad. Sci. 105, 17442–17446.

Bellwood, D.R., Hughes, T.P., Folke, C., Nyström, M., 2004. Confronting the coral reef crisis. Nature. 429, 827–833.

Berkelmans, R., Van Oppen, M.J.H., 2006. The role of zooxanthellae in the thermal tolerance of corals: a 'nugget of hope'for coral reefs in an era of climate change. Proc. R. Lond. B. 273, 2305–2312.

Bruno, J.F., Edmunds, P.J., 1997. Clonal variation for phenotypic plasticity in the coral *Madracis mirabilis*. Ecology 78, 2177–2190.

Bruno, J.F., Edmunds, P.J., 1998. Metabolic consequences of phenotypic plasticity in the coral *Madracis mirabilis* (Duchassaing and Michelotti): The effect of morphology and water flow on aggregate respiration. J. Exp. Mar. Biol. Ecol. 229, 187–195.

Chan, N., Connolly, S.R., 2013. Sensitivity of coral calcification to ocean acidification: a meta-analysis. Glob. Chang. Biol. 19, 282–290.

Cohen, A.L., Holcomb, M., 2009. Why coral care about ocean acidification: uncovering the mechanism. Oceanogr. 22, 118–127.

Comeau, S., Edmunds, P.J., Spindel, N.B., Carpenter, R.C., 2013a. The responses of eight coral reef calcifiers to increasing partial pressure of CO_2 do not exhibit a tipping point. Limnol. Oceanogr. 58, 388–398.

Comeau, S., Carpenter, R.C., Edmunds, P.J., 2013b. Effects of feeding and light intensity on the responses of the coral *Porites rus* to ocean acidification. Mar. Biol. 160, 1127–1134.

Comeau, S., Edmunds, P.J., Spindel, N.B., Carpenter, R.C., 2014. Fast coral reef calcifiers are more sensitive to ocean acidification in short-term laboratory incubations. Limnol. Oceanogr. 59, 1081–1091.

Darling, E.S., Alvarez-Filip, L., Oliver, T.A., McClanahan, T.R., Côté, 2012. Evaluating life-history strategies of reef corals from species traits. Ecol. Lett. 15, 1378–1386.

Davies, S.P., 1989. Short-term growth measurements of corals using an accurate buoyant weighing technique. Mar. Biol. 101, 389–395.

De'ath, G., Fabricius, K.E., Sweatman, H., Puotinen, M., 2012. The 27–year decline of coral cover on the Great Barrier Reef and its causes. Proc. Natl. Acad. Sci. 109, 17995–17999.

Dickson, A.G., Sabine, C.L., Christian, J.R., 2007. Guide to best practices for ocean CO_2 measurements PICES Special Publication. 3. PICES, Sidney, BC.

Doney, S.C., Fabry, V.J., Feely, R.A., Kleypas, J.A., 2009. Ocean acidification: The other CO_2 problem. Annu. Rev. Mar. Sci. 1, 169–192.

Edmunds, P.J., 2011. Zooplanktivory ameliorates the effects of ocean acidification on the reef coral *Porites* spp. Limnol. Oceanogr. 56, 2402–2410.

Edmunds, P.J., 2016. MCR LTER: Coral Reef: Long-term Population and Community Dynamics: Corals. http://dx.doi.org/10.6073/pasta/1f05f1f52a2759dc096da9c24e88b1e8 ongoing since 2005. knb-lter-mcr.4.33.

Edmunds, P.J., Gates, R.D., 2008. Acclimatization in tropical reef corals. Mar. Ecol. Prog. Ser. 361, 307–310.

Edmunds, P.J., Brown, D.B., Moriarty, V.M., 2012. Interactive effects of ocean acidification and temerpature on two scleractinian corals from Moorea, French Polynesia. Glob. Chang. Biol. 18, 2173–2183.

Edmunds, P.J., Adjeroud, M., Baskett, M.L., Baums, I.B., Budd, A.F., Carpenter, R.C., Fabina, N.S., Fan, T.Y., Franklin, E.C., Gross, K., Han, X., 2014. Persistence and change in community composition of reef corals through present, past, and future climates. PloS one. 9, e107525.

Feely, R.A., Doney, S.C., Cooley, S.R., 2009. Ocean acidification: present conditions and future changes in a high-CO2 world.". Oceanogr. 22, 36–47.

Franklin, E.C., Stat, M., Pochon, X., Putnam, H.M., Gates, R.D., 2011. GeoSymbio: a hybrid, cloud-based web application of global geospatial bioinformatics and ecoinformatics for Symbiodinium–host symbioses. Mol. Ecol. Resour. 12, 369–373.

Graham, N.A.J., Wilson, S.K., Jennings, S., Polunin, N.V., Bijoux, J.P., Robinson, J., 2006. Dynamic fragility of oceanic coral reef ecosystems. Proc. Natl. Acad. Sci. 103, 8425–8429.

Hoegh-Guldberg, O., Mumby, P., Hooten, A., Steneck, R., Greenfield, P., Gomez, E., Harvell, C., Sale, P., Edwards, A., Caldeira, K., Knowlton, N., Eakin, C., Iglesias-Prieto, R., Muthiga, N., Bradbury, R., Dubo, A., Hatziolos, M., 2007. Coral reefs under rapid climate change and ocean acidfication. Science 318, 1737–1742.

Hoenig, J.M., Heisey, D.M., 2001. The abuse of power. Am. Stat. 55, 19–24.

Hoogenboom, M.O., Connolly, S.R., Anthony, K.R., 2008. Interactions between morphological and physiological plasticity optimize energy acquisition in corals. Ecology 89, 1144–1154.

Jackson, J.B.C., 1979. Morphological strategies of sessile organisms. In: Larwood, G.P., Rosen, B.R. (Eds.), Biology and Systematics of Colonial Organisms. Academic Press, London, pp. 499–555.

Jackson, J.B.C., Donovan, M., Cramer, K., Lam, V., 2014. Status and Trends of Caribbean Coral Reefs: 1980–2012. Global Coral Reef Monitoring Network.

Jaubert, J., 1977. Light, metabolism, and growth forms of the hermatypic scleractinian coral *Synarea convexa* Verill in the lagoon of Moorea (French Polynesia). Proc. 3rd Int. Coral Reef Symp. 483–488.

Kroeker, K.J., Kordas, R.L., Crim, R.N., Singh, G.G., 2010. Meta-analysis reveals negative yet variable effects of ocean acidification on marine organisms. Ecol. Lett. 13, 1419–1434.

Kroeker, K.J., Kordas, R.L., Crim, R., Hendriks, I.E., Ramajo, L., Singh, G.S., Duarte, C.M., Gattuso, J.P., 2013. Impacts of ocean acidification on marine organisms: quantifying sensitivies and interactions with warming. Glob. Chang. Biol. 19, 1884–1894.

Lavigne, H., Gattuso, J.P., 2012. seacarb: seawater carbonate chemistry with R, R package version 2.4.6. http://CRAN.Rproject.org/package=seacarb.

Lesser, M.P., Weis, V.M., Patterson, M.R., Jokiel, P.L., 1994. Effects of morphology and water motion on carbon delivery and productivity in the reef coral, *Pocillopora damicornis* (Linnaeus): diffusion barriers, inorganic carbon limitation, and biochemical plasticity. J. Exp. Mar. Biol. Ecol. 178, 153–179.

Loya, Y., Sakai, K., Yamazato, K., Nakano, Y., Sambali, H., van Woesik, R., 2001. Coral bleaching: the winners and losers. Ecol. Lett. 4, 122–131.

Marsh, J.A., 1970. Primary productivity of reef-building calcareous red algae. Ecology 51, 255–263.

McClanahan, T., Polunin, N., Done, T., 2002. Ecological states and the resilience of coral reefs. Cons. Ecol. 6, 18 [online] URL: http://www.consecol.org/vol6/iss2/art18/.

Moss, R.H., Edmonds, J.A., Hibbard, K.A., Manning, M.R., Rose, S.K., van Vuuren, D.P., Carter, T.R., Emori, S., Kainuma, M., Kram, T., Meehl, G.A., Mitchell, J.F.B., Nakicenovic, N., Riahi, K., Smith, S.J., Stouffer, R.J., Thomson, A.M., Weyant, J.P., Wilbanks, T.J., 2010. The next generation of scenarios for climate change research and assessment. Nature 463, 747–756.

Okazaki, R.R., Towle, E.K., van Hooidonk, R., Mor, C., Winter, R.N., Piggot, A.M., Cunning, R., Baker, A.C., Klaus, J.S., Swart, P.K., Langdon, C., 2016. Species-specific responses to climate change and community composition determine future calcification rates of Florida Keys reefs. Glob. Chang. Biol. http://dx.doi.org/10.1111/gcb.13481.

Padillo-Gamiño, J.L., Hanson, K.M., Stat, M., Gates, R., 2012. Phenotypic plasticity of the coral *Porites rus*: acclimatization responses to a turbid environment. J. Exp. Mar. Biol. Ecol. 434, 71–80.

Patterson, M., 1992. A chemical engineering view of cnidarian symbioses. Am. Zool. 32, 566–582.

Putnam, H.M., Edmunds, P.J., 2011. The physiological response of reef corals to diel fluctuations in seawater temperature. J. Exp. Mar. Biol. Ecol. 396, 216–223.

Putnam, H.M., et al., 2012. Endosymbiotic flexibility associates with environmental sensitivity in scleractinian corals. Proc. R. Lond. B. http://dx.doi.org/10.1098/rspb.2012.1454.

Quinn, G.P., Keough, M.J., 2002. Experimental Design and Data Analysis for Biologists. Cambridge University Press, Melbourne.

Rosengberg, E., Koren, O., Reshef, L., Efrony, R., Zilber-Rosenberg, I., 2007. The role of microorganisms in coral health, disease and evolution. Nat. Rev. Microbiol. 5, 355–362.

Silbiger, N.J., Guadayol, Ò., Thomas, F.I., Donahue, M.J., 2014. Reefs shift from net accretion to net erosion along a natural environmental gradient. Mar. Ecol. Prog. Ser. 515, 33–44.

Tambutté, E., Venn, A.A., Holcomb, M., Segonds, N., Techer, N., Zoccola, D., Allemand, D., Tambutté, S., 2015. Morphological plasticity of the coral skeleton under CO_2-driven seawater acidification. Nat. Comm. http://dx.doi.org/10.1038/ncomms8368.

Todd, P., 2008. Morphological plasticity in scleractinian corals. Biol. Rev. 83, 315–337.

van Woesik, R., Sakai, K., Ganase, A., Loya, Y., 2011. Revisiting the winners and the losers a decade after coral bleaching. Mar. Ecol. Prog. Ser. 434, 67–76.

Vermeij, M.A., Bak, R.P.M., 2002. How are coral population structured by light? Marine light regimes and the distribution of *Madracis*. Mar. Ecol. Prog. Ser. 233, 105–116.